



Physiologic compliance in engineered small-diameter arterial constructs based on an elastomeric substrate

Peter M. Crapo¹, Yadong Wang*

Wallace H. Coulter Department of Biomedical Engineering, Georgia Institute of Technology, Atlanta, GA 30332, USA

ARTICLE INFO

Article history:

Received 25 September 2009

Accepted 14 November 2009

Available online 3 December 2009

Keywords:

Arterial tissue engineering

Vascular compliance

Elastin

Poly(glycerol sebacate)

Small-diameter vascular grafts

ABSTRACT

Compliance mismatch is a significant challenge to long-term patency in small-diameter bypass grafts because it causes intimal hyperplasia and ultimately graft occlusion. Current engineered grafts are typically stiff with high burst pressure but low compliance and low elastin expression. We postulated that engineering small arteries on elastomeric scaffolds under dynamic mechanical stimulation would result in strong and compliant arterial constructs. This study compares properties of engineered arterial constructs based on biodegradable polyester scaffolds composed of either rigid poly(lactide-co-glycolide) (PLGA) or elastomeric poly(glycerol sebacate) (PGS). Adult baboon arterial smooth muscle cells (SMCs) were cultured *in vitro* for 10 days in tubular, porous scaffolds. Scaffolds were significantly stronger after culture regardless of material, but the elastic modulus of PLGA constructs was an order of magnitude greater than that of porcine carotid arteries and PGS constructs. Deformation was elastic in PGS constructs and carotid arteries but plastic in PLGA constructs. Compliance of arteries and PGS constructs were equivalent at pressures tested. Altering scaffold material from PLGA to PGS significantly decreased collagen content and significantly increased insoluble elastin content in constructs without affecting soluble elastin concentration in the culture medium. PLGA constructs contained no appreciable insoluble elastin. This research demonstrates that: (1) substrate stiffness directly affects *in vitro* tissue development and mechanical properties; (2) rigid materials likely inhibit elastin incorporation into the extracellular matrix of engineered arterial tissues; and (3) grafts with physiologic compliance and significant elastin content can be engineered *in vitro* after only days of cell culture.

© 2009 Elsevier Ltd. All rights reserved.

1. Introduction

Coronary heart disease is the leading cause of death in the U.S., with an estimated annual cost exceeding \$150 billion [1]. Approximately half-a-million coronary artery bypass graft procedures and an even greater number of percutaneous arterial procedures (coronary angioplasty, stent revascularization, endarterectomy, etc.) are performed annually. Coronary artery bypass is associated with better outcomes compared to percutaneous procedures [2]. The internal thoracic artery is the benchmark for coronary bypass, but its use is limited by issues of accessibility and length [3]. Saphenous vein grafts are easiest to access and have the least

impact on tissue morbidity and patient health. However, saphenous vein grafts used for coronary bypass occlude at much higher rates (~50% within 10 years) compared to arterial grafts [4], underscoring the need to match the biological and mechanical properties of the specific artery being replaced. Compliance mismatch influences a variety of flow and wall shear stress parameters, which in turn regulate complex biological responses to determine vascular remodeling outcomes such as restenosis, intimal hyperplasia, and occlusion [5].

Compliance mismatch results in intimal hyperplasia at the downstream anastomosis [6]. It has been suggested that increased shear stress as a result of compliance mismatch is the root cause of graft-associated intimal hyperplasia [7,8]. The importance of compliance matching was first established by Abbott et al. using a canine model to investigate compliance [9]. Canine carotid artery autografts and femoral arteries were either compliance-matched (1:1) or mismatched (2:5), resulting in patencies of 85% or 37% at 90 days post-implantation, respectively. Interestingly, Sonoda et al. achieved a patency rate similar to that of Abbot et al. (86%, also in canine common carotid) at 365 days post-implantation using

* Corresponding author. Department of Bioengineering, McGowan Institute, University of Pittsburgh, 300 Technology Drive, Pittsburgh, PA 15219, USA. Tel.: +1 412 624 7196; fax: +1 412 383 8788.

E-mail addresses: pcrapo@exponent.com (P.M. Crapo), yaw20@pitt.edu (Y. Wang).

¹ Current address: Exponent Failure Analysis Associates, 5401 McConnell Avenue, Los Angeles, CA 90066, USA. Tel.: +1 310 754 2738; fax: +1 310 754 2799.

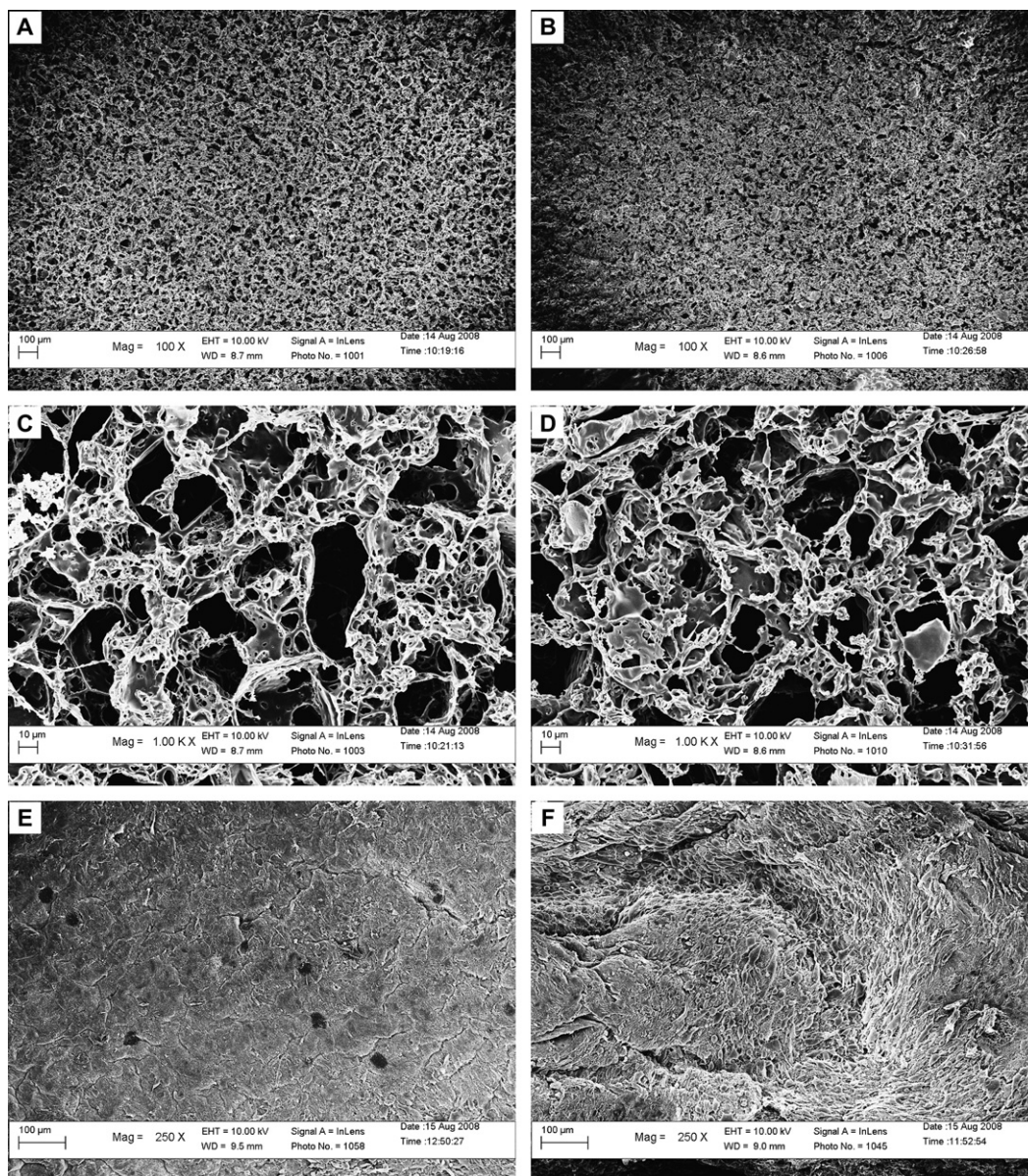


Fig. 1. Electron micrographs of scaffold luminal microstructure and cellular luminal confluence. Luminal surfaces appeared similar in micrographs of (A) PGS and (B) PLGA scaffolds (scale bars = 100 µm). Luminal microstructure also appeared similar in high-magnification micrographs of (C) PGS and (D) PLGA scaffolds (scale bars = 10 µm). Cellular confluence appeared equivalent on the luminal surfaces of (E) PGS and (F) PLGA arterial constructs cultured with adult baboon arterial SMCs for 10 days. Topography varied due to scaffold compaction and individual SMCs were visible on their luminal surfaces in some locations. Dark spots (E) are charging artifacts.

biodegradable poly(urethane)/crosslinked gelatin grafts with physiologic compliance [10].

In contrast to these studies, abluminal constraint of canine common iliac artery sections suggested that compliance mismatch alone does not cause intimal hyperplasia [11]. Flow irregularities at the downstream anastomosis influence protein transport [12] and are likely to contribute to intimal hyperplasia by increasing residence time of chemotactic factors [13] and the concentration of growth factors associated with intimal hyperplasia and atherosclerosis as well as mitogenic factors associated with higher cell proliferation [14]. Additionally, compliance mismatch increases suture line stresses at anastomoses. Considered collectively, these results indicate the importance of compliance matching for vascular graft patency.

An extracorporeal source of small-diameter (<5 mm) non-thrombogenic vascular grafts possessing physiologic compliance would prevent the harvesting of multiple native vessels when

unfavorable remodeling occurs and would provide an alternative when autologous grafts are unavailable. However, current engineered grafts are challenged by compliance mismatch and thrombosis, resulting in undesirable tissue remodeling and graft occlusion.

Artificial grafts have been engineered with super-physiologic burst pressures [15–20] and *in vivo* patency rates of ~80% at time points beyond three months [15,17,18,21], indicating that aneurysm and thrombosis, challenges which cause graft failure in the short-term, are being overcome. However, research efforts have not yet produced an engineered graft with physiologic compliance. Elastomer-based grafts may facilitate compliance matching, thereby improving long-term patency rates for engineered vasculature. We have previously developed [22] and improved [23] a method to fabricate tubular, porous scaffolds from a biodegradable elastomer, poly(glycerol sebacate) (PGS), and shown that adult baboon arterial smooth muscle cells (SMCs) cultured on PGS proliferate and

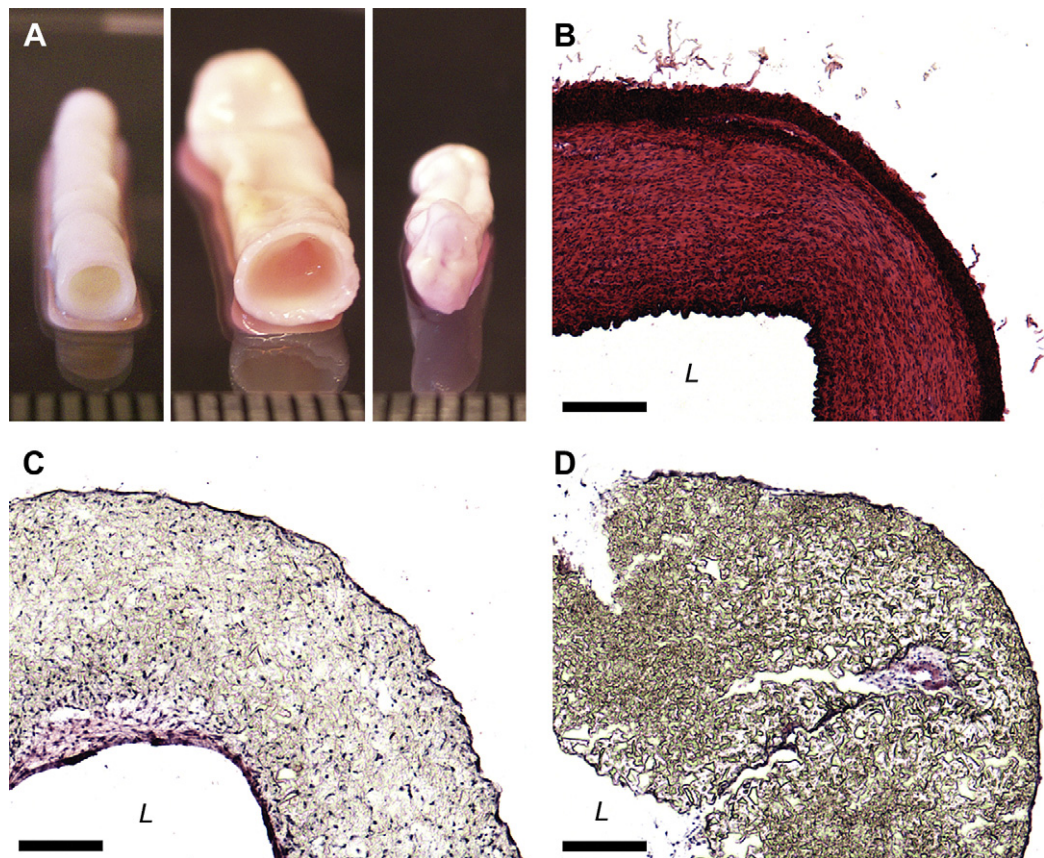


Fig. 2. Macroscopic and histological appearance of arteries and engineered arterial constructs. Macroscopic appearance of (A) the *tunica media* and *intima* of a porcine carotid artery, a PGS construct, and a PLGA construct (shown left to right). Staining with H&E to qualitatively assess cell and protein distribution showed that (B) porcine carotid arteries were dense and highly organized while (C) PGS constructs and (D) PLGA constructs had concentrations of cells and proteins at the luminal and abluminal surfaces and cells distributed throughout the scaffold walls. Ruler divisions = 1.0 mm and scale bars = 250 μm , L = lumen. For images of complete histological cross-sections see Fig. S6.

maintain their phenotype [24]. Additionally, we have demonstrated the ability of PGS scaffolds to support co-expression of elastin and collagen by adult SMCs in three-dimensional *in vitro* culture, resulting in highly distensible engineered tissues [25].

We hypothesized that grafts engineered from compliant materials and adult vascular SMCs under biomimetic *in vitro* culture conditions could develop compliance comparable to autologous arteries. To test our hypothesis, constructs were created from tubular, porous scaffolds composed of PGS or the benchmark biomaterial poly(lactide-co-glycolide) (PLGA), each cultured with SMCs under identical conditions. PLGA was chosen based on its similarities to PGS: both are biodegradable polyesters with no known bioactivity, and both generate carboxylic acid and alcohol upon hydrolysis. Although PLGA and PGS differ in hydrophilicity, and therefore initial surface protein adsorption from culture medium is likely different, this difference is expected to be attenuated during culture by cell-dominated protein deposition on scaffold surfaces. The critical difference between PLGA and PGS is therefore elasticity; PLGA is a rigid material, whereas PGS is a compliant elastomer with mechanical properties that more closely match the properties of cardiovascular tissues [26–28].

2. Materials and methods

2.1. Overall approach to scaffold fabrication

Scaffolds were fabricated from PGS [26] synthesized in-house [22] or from PLGA (5050 DLG 5E; Lakeshore Biomaterials, Birmingham, AL, USA) using a solvent casting and particulate leaching process [23,29]. Sodium chloride (EMD Chemicals, Gibbstown, NJ, USA) was ground and sieved to select salt particles with a size range of

75–90 μm as porogens. Two new methods of PGS scaffold fabrication were developed to reduce scaffold geometric and mechanical tolerances and decrease scaffold wall thickness. The new methods were compared to a high-yield method previously developed [23]. PGS and PLGA scaffolds selected for cell culture were fabricated using only the most advantageous method.

2.2. Methods of scaffold fabrication

The previous scaffold fabrication method [23] (denoted as type A scaffolds) used in-house bifurcated poly(tetrafluoroethylene) (PTFE) molds with a cylindrical recess (ID 7.94 mm, length 60 mm). Salt particles were added between the larger recess and a heat-shrinkable mandrel (OD 5.28 mm, ID 4.76 mm). Lecithin mold release (Diversified Brands, Cleveland, OH, USA) was applied to all salt-contacting mold surfaces prior to assembly and salt loading through a slot in the center of one half. Salt was fused at 88% humidity and 37 °C for 6.5 h.

The second scaffold fabrication method (denoted as type B scaffolds) replaced the bifurcated outer mold with a 90-mm length of PTFE tubing (OD 12.7 mm, ID 7.94 mm; McMaster-Carr, Aurora, OH, USA) coated with lecithin mold release. Spacing and concentricity between the outer PTFE tubing and the mandrel was maintained by a ring of PTFE tubing (OD 7.94 mm, ID 4.76 mm, 1.0 mm length; McMaster-Carr) with four non-contiguous sections of its outer diameter cut away for ventilation. Salt was loaded into the vertical mold assembly with the spacer ring at its bottom while the upper end of the mandrel was manually centered. Salt was fused at 88% humidity and 37 °C for 6.5 h.

The third scaffold fabrication method (denoted as type C scaffolds) replaced the outer PTFE tubing with a 70-mm length of glass tubing (OD 9.0 mm, wall thickness 1.0 mm; Small Parts, Miramar, FL, USA) coated on the inner surface with 1.0% hyaluronic acid (HA; Sigma-Aldrich, St. Louis, MO, USA), which was dried overnight at 37 °C and 100 mTorr. The heat-shrinkable mandrel, spacer ring, and salt loading were the same as in the second method. Salt was fused at 88% humidity and 37 °C for 20 min. A briefer fusion period was likely required because the hyaluronic acid accelerated moisture sequestration.

Salt templates were dried overnight at 37 °C and 100 mTorr regardless of method. Heat-shrinkable mandrels were removed at 120 °C for 5 min. Salt templates remained in the outer molds during polymer addition for type B or C scaffolds. PGS

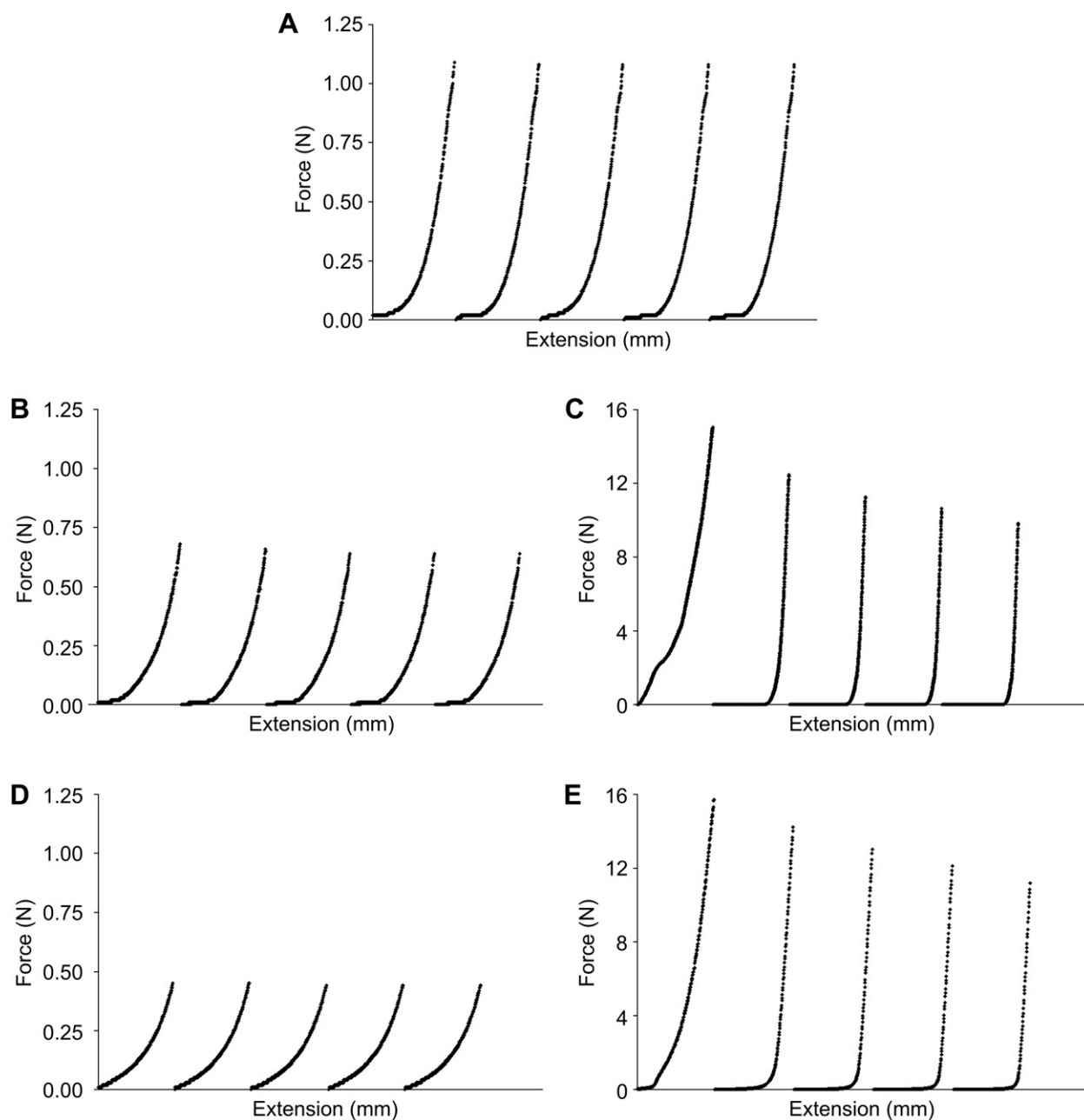


Fig. 3. Deformation and elastic recovery of arteries and engineered arterial constructs in transverse compression. Segments of porcine carotid arteries, PGS or PLGA constructs, and PGS or PLGA scaffolds were compressed perpendicular to their axis. Five force–extension cycles are shown chronologically for each tested segment. Elastic recovery was observed in (A) arteries and (B) PGS constructs, while plastic deformation was observed in (C) PLGA constructs. Scaffolds composed of (D) PGS or (E) PLGA showed similar behavior to their construct counterparts with or without degradation (degraded scaffold data not shown). Increases in moduli caused by ECM production were evident from steeper regions near the end of the force–extension curves of (B) PGS constructs compared to (D) PGS scaffolds and a notable difference in the toe regions and near the end of the force–extension curves of (B) PLGA constructs compared to (D) PLGA scaffolds (see also Fig. 4). The *tunica adventitia* of arteries was removed prior to testing.

pre-polymer or PLGA was dissolved in tetrahydrofuran at a mass ratio of 1:5 and added at 4.0 mg polymer per mm salt template length. Tetrahydrofuran was allowed to evaporate for at least one hour. PGS was cured at 150 °C and 100 mTorr for 24 h. PLGA was placed overnight in a vacuum oven (20 °C, 100 mTorr) to remove all THF. A series of two water baths (first bath ~24 h, second bath >48 h) was used to dissolve the salt template and release type B or C polymer tubes from their molds. Individual scaffolds were obtained by bisecting the tubes into 30-mm sections. Scaffolds were lyophilized and stored dry.

2.3. Scaffold evaluation

The percentage of usable scaffolds (yield) and scaffold dimensions, micro-structure, porosity, and mechanical properties were determined as previously described [23]. Scaffolds that were free of through-cracks and holes along their entire length were considered usable. Scaffold wall thickness was measured at eight

evenly spaced locations around the circumference of 5-mm scaffold segments. Randomly selected scaffold cross-sections and lumens were sputter-coated with gold and observed via scanning electron microscope. Porosity was calculated using an ethanol displacement method previously described [30]. Porosity measurements of two 5.0-mm type C scaffold segments by micro-computed tomography [31] fell within one standard deviation of the mean as calculated from ethanol submersion data, but micro-computed tomography was not used to evaluate porosity due to prohibitive time and cost requirements.

Scaffolds were cut into 5-mm segments and tested to failure under uniaxial tension (tension perpendicular to the segment axis) at 0.20 mm/s after soaking for 24 h in PBS [23]. Ultimate tensile stress was calculated from maximum force and wall cross-sectional area. Strain at failure was calculated from the change in luminal circumference normalized by initial circumference. Stress and strain at intermediate points were calculated to determine each segment's linear elastic modulus in the linear stress–strain region of 40–80% of the ultimate tensile stress.

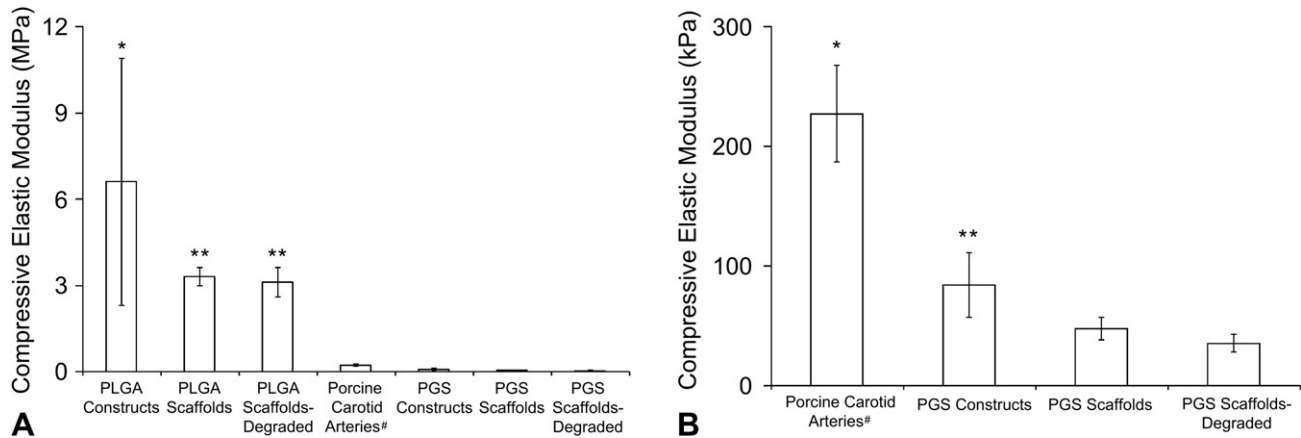


Fig. 4. Elastic moduli of arteries and engineered arterial constructs. Segments of porcine carotid arteries, PGS or PLGA constructs, and PGS or PLGA scaffolds with or without degradation were compressed perpendicular to their axis. Transverse compressive elastic moduli (E_c) were determined from the second, third, and fourth force-extension cycles to 50% strain. (A) Comparison of all experimental groups and controls ($n = 12, 12, 12, 8, 10, 12$, and 12 from left to right). * E_c of PLGA constructs was significantly higher than all other groups. ** E_c of undegraded and degraded PLGA scaffolds were significantly higher than E_c of porcine carotid arteries and all PGS groups. (B) Comparison of positive control and PGS groups only. * E_c of arteries was significantly higher than all PGS groups. ** E_c of PGS constructs was significantly higher than E_c of undegraded and degraded PGS scaffolds. #The *tunica adventitia* of arteries was removed prior to testing.

To compare polymer degradation rates, PGS or PLGA type C scaffolds were cut into 5-mm segments, placed in pre-weighed microcentrifuge tubes, sterilized by steam autoclaving for PGS (15 min at 150 °C) or ethylene oxide gas for PLGA (>72 h of subsequent outgassing), and weighed. Complete culture medium was added (2.00 ml per tube) followed by horizontal rotation at 2.0 rpm and 37 °C for 10 days. The ratios of surface area to volume for degraded scaffold segments and scaffolds in culture were identical (80 mm² per ml). After transverse compression testing (see Section 2.7), scaffold segments were returned to their tubes, frozen, lyophilized, and re-weighed. Pre-weighed microcentrifuge tubes containing only 2.00 ml complete culture medium were likewise frozen, lyophilized, and re-weighed as a control.

Note: Based on scaffold evaluation results, only type C scaffolds were used for cell culture to create engineered arterial constructs.

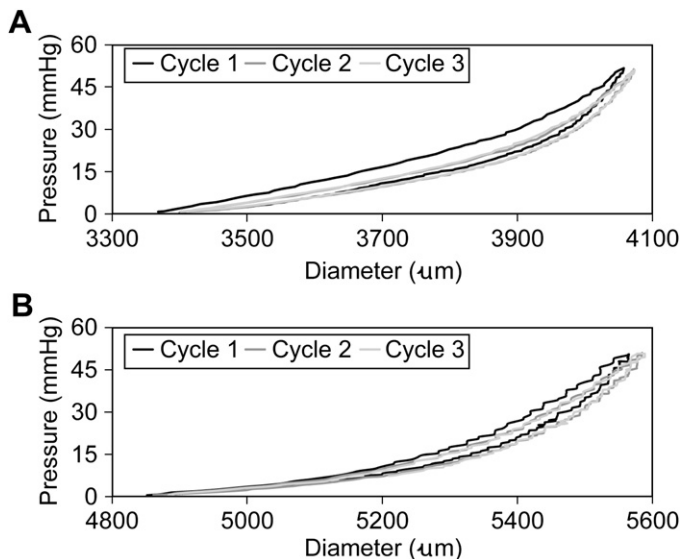


Fig. 5. Elastic recovery of arteries and engineered arterial constructs. Segments of porcine carotid arteries and whole PGS constructs were pressure-diameter tested for comparison. Constructs were cycled to each target pressure three times, with hysteresis observed only during the first cycle. Complete elastic recovery was observed after the initial cycle to each target pressure in (A) porcine carotid arteries up to and including the highest pressure tested (240 mmHg) and in (B) PGS constructs up to pressures near their burst pressure (cycles to 50 mmHg are shown for a construct with a burst pressure of 56 mmHg). The *tunica adventitia* of porcine carotid arteries was removed prior to testing.

2.4. Cell culture

A pulsatile perfusion bioreactor was designed for culturing vascular cells on tubular porous scaffolds *in vitro* as previously described [23,25]. The bioreactor included four medium reservoirs, eight flow circuits (two per reservoir) comprised of silicone tubing with coiled sections for gas exchange, scaffold-containing chambers with shorter silicone tubing assemblies that could be detached from the bulk of each circuit, and additional silicone tubing to return medium to the reservoirs. Flow was driven and controlled by a Masterflex L/S pump (model 77301-22; Cole-Parmer Instrument Company, Vernon Hills, IL).

Smooth muscle cells (SMCs) were isolated from the carotid arteries of juvenile male baboons (*Papio anubis*) and characterized in two-dimensional culture prior to passaging and seeding [24]. Complete culture medium contained MCDB 131 with 10% irradiated FBS, 1.0% L-glutamine, and 50 mcg/ml ascorbic acid, with 100 IU/ml penicillin, 100 mcg/ml streptomycin, and 0.25 mcg/ml amphotericin B as antibiotics and antimycotic.

PGS scaffolds were aligned with the luminal tubing of their chambers using 1.0-mm bands of heat-shrinkable food-grade acrylated poly(olefin) (OD 6.88 mm, ID 6.35 mm; McMaster-Carr) shrunk around each end of the scaffold by heating at 120 °C. PLGA scaffolds were aligned with the luminal tubing of their chambers using 1.0-mm bands of silicone tubing (OD 6.35 mm, ID 3.18 mm; McMaster-Carr) abutting each end of the scaffold.

In preparation for cell seeding, scaffolds attached to their chambers were sterilized (same method as was used for the degradation study: steam for PGS or ethylene oxide gas for PLGA) and pretreated with a series of perfusions at 1.0 ml/min to remove any unreacted monomers and oligomers and residual salt prior to cell seeding: 70% ethanol for 1 h, 50% ethanol for 1 h, 25% ethanol for 1 h, and PBS for 2 h. During 30 min of perfusion with each pretreatment fluid, flow was forced through the scaffold wall by clamping the luminal tubing outlet. Scaffolds were then conditioned with complete culture medium for 24 h.

Each scaffold within its chamber was detached from its flow circuit, and SMCs (passage 5) were seeded in the scaffold lumen (2.0 × 10⁶ SMCs per cm² of luminal surface area) followed by four hours of horizontal rotation. Reservoirs received fresh medium (250 ml per reservoir), scaffold chambers were reattached to their flow circuits, and through-wall perfusion was resumed at 1.0 ml/min for 15 min followed by luminal flow. The flow rate was increased steadily from 1.0 ml/min (1.1 dynes/cm²) on day one to 10 ml/min (11 dynes/cm²) on day 10, the termination point of the study. Medium was changed on day seven, and additional ascorbic acid (50 mcg/ml) was injected into each medium reservoir on days three and five.

2.5. Positive control

The left and right common carotid arteries of Large White/Yorkshire pigs (~30 kg, *Sus scrofa domestica*) were excised immediately following anesthesia (intravenous ketamine and xylazine) and euthanasia (intravenous pentobarbital) in accordance with the Georgia Institute of Technology's Institutional Animal Care and Use Committee guidelines and with their approval. Each artery was rinsed in HBSS and the *tunica adventitia* was removed using scissors and a scalpel, leaving the *tunica media* and *tunica intima* intact. Porcine arteries were selected as controls because of the limited availability of baboon arteries.

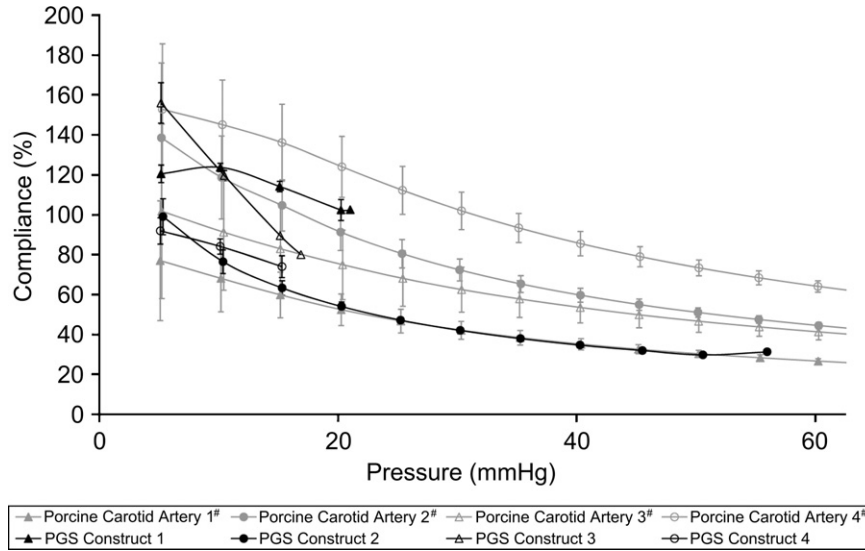


Fig. 6. Physiologic compliance of arteries and engineered arterial constructs. The compliance of porcine carotid arteries (gray, $n=4$) and PGS constructs (black, $n=4$) was remarkably similar at the pressures tested. There was no statistical difference between the two groups. PGS scaffolds hold no pressure due to their high porosity. #The *tunica adventitia* of porcine carotid arteries was removed prior to testing.

2.6. Histology

A short segment of each artery and cultured PGS or PLGA scaffold (designated respectively as PGS or PLGA constructs) did not undergo mechanical or biological testing and was instead snap-frozen, cryosectioned, and stained with hematoxylin and eosin.

2.7. Mechanical evaluation of engineered arterial constructs

Only PGS constructs and artery segments of similar length underwent pressure–diameter testing. The brittle nature of PLGA constructs prevented cannulation and attachment to pressure–diameter testing apparatus. PGS constructs were tested to burst and arteries were tested to the maximum pressure of the system (200 mmHg). Vessels were attached to a flow circuit, submerged in and perfused with medium, and stretched to $\lambda = 1.2$ (120% of length prior to attachment). Luminal pressure was cycled between zero and a target pressure, which was incrementally increased by 5 mmHg after three cycles to each target (rate of increase ~ 60 mmHg/min and rate of decrease ~ 40 mmHg/min). Pressure was dynamically controlled using LabVIEW (National Instruments, Austin, TX) and recorded at 0.25–1.0 Hz while vessel diameter was observed via light microscopy, with images of the external diameter recorded and the diameter measured synchronously with pressure. Pressure–diameter data were used to determine elastic recovery and compliance of arteries and constructs. Mean diameter was calculated along a portion of the vessel length

from image data. Compliance was defined as the inverse of Peterson’s elastic modulus according to the following equation: $C = (\Delta D/D_0)/\Delta P$ [32].

Scaffold, construct, and artery segments (length ~ 5 mm) were tested to 50% strain in transverse compression (planar compression perpendicular to the segment axis) at 0.0167 mm/s. Undegraded scaffold segments were tested after soaking for 24 h in PBS. Segments were pre-cycled to 5.0% strain approximately five times until load stabilized at ~ 0.05 N (range 0.02–0.10 N). Five compression cycles to 50% strain (ϵ_{Fmax}) were completed in rapid succession followed by image-based measurements of post-compression segment cross-sectional area (A_c). Only artery segments recovered to their original cylindrical geometry after testing, and A_c for artery segments was therefore multiplied by a correction factor of $\pi/2$. Elastic recovery was determined by comparing force–extension curves and the maximum compressive force (F_{max}) for each segment’s five-cycle compression series. The strain at half-maximum force ($\epsilon_{0.5Fmax}$) and F_{max} were taken directly from the raw data. The compressive modulus of elasticity (E_c) for the segment was taken as the mean of E_c for cycles 2–4, which were calculated according to the following equation: $E_c = (0.50F_{max}/A_c)/(\epsilon_{Fmax} - \epsilon_{0.5Fmax})$.

2.8. Biological evaluation of engineered arterial constructs

Collagen content was evaluated by measuring hydroxyproline content similar to previously reported methods using chloramine T [33,34]. A hydroxyproline standard

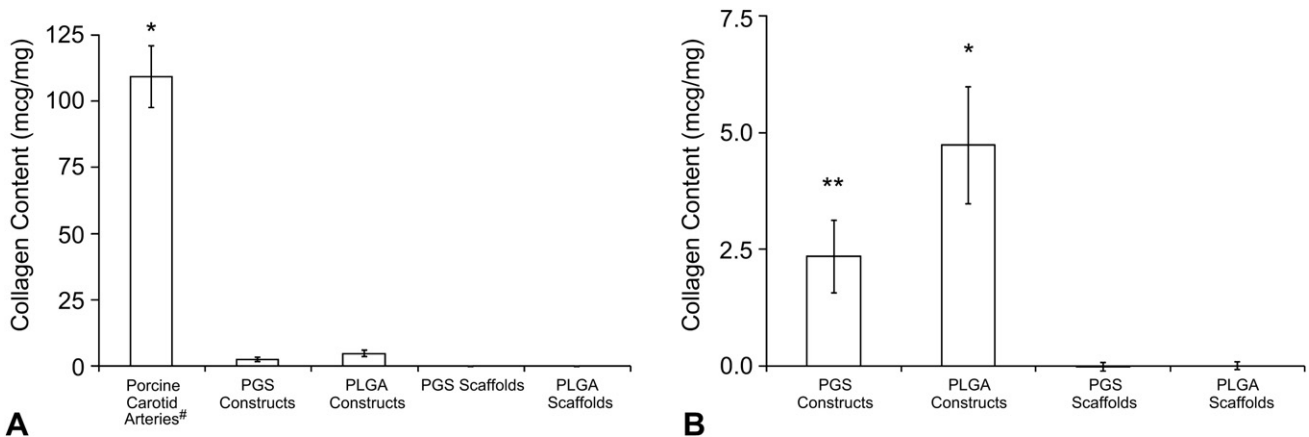


Fig. 7. Total collagen content in arteries and engineered arterial constructs. Total collagen contents in porcine carotid arteries, PGS or PLGA constructs, and PGS or PLGA scaffolds were measured per unit wet weight by quantifying 4-hydroxyproline content. (A) Comparison of experimental groups and controls ($n = 4, 4, 4, 8,$ and 8 from left to right). *Porcine carotid arteries contained significantly more collagen than all other groups. (B) Comparison of experimental groups and negative controls only. *PLGA constructs contained significantly more collagen than PGS constructs and uncultured scaffolds. **PGS constructs contained significantly more collagen than uncultured scaffolds. #The *tunica adventitia* of porcine carotid arteries was removed prior to testing.

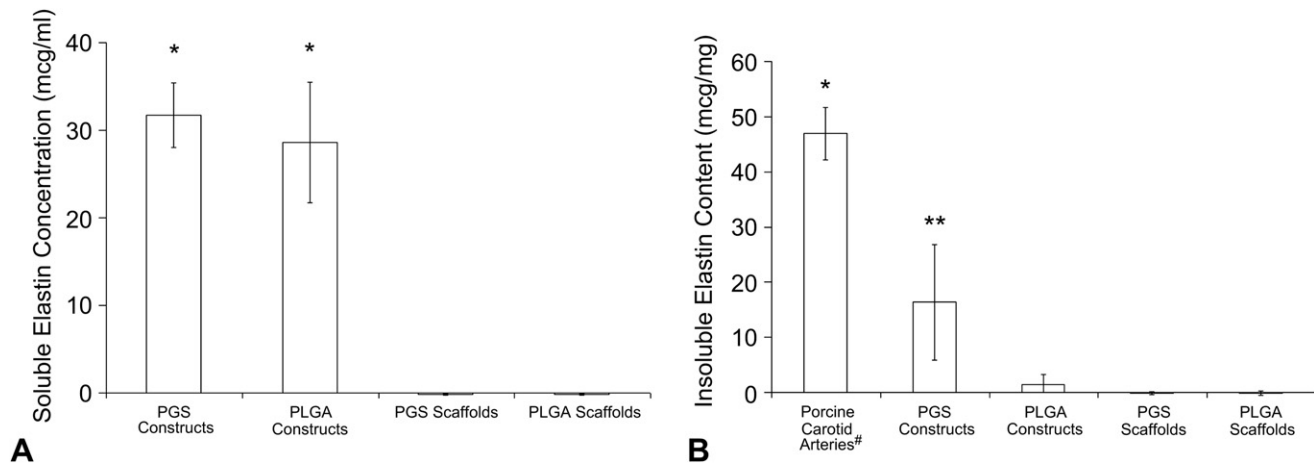


Fig. 8. Elastin in arteries and engineered arterial constructs. Elastin production was quantified using an elastin-binding dye. (A) Soluble elastin concentrations in culture medium collected at the termination of culture of PGS or PLGA constructs were measured after centrifugation to remove any insoluble elastin ($n = 4, 4, 10,$ and 10 from left to right). *PGS and PLGA constructs released significant amounts of soluble elastin into culture medium. (B) Insoluble elastin contents in porcine carotid arteries, PGS or PLGA constructs, and PGS or PLGA scaffolds were measured per unit wet weight after acid hydrolysis of each construct, which destroyed all proteins except elastin, and centrifugation to pellet insolubles ($n = 4, 4, 4, 9,$ and 9 from left to right). *Arteries contained significantly more insoluble elastin than all other groups. ** PGS constructs contained significantly more insoluble elastin than PLGA constructs and uncultured scaffolds, but PLGA constructs did not contain significantly more insoluble elastin compared to uncultured scaffolds (even if the positive control was excluded). [#]The *tunica adventitia* of porcine carotid arteries was removed prior to testing.

was prepared in duplicate by dissolving L-hydroxyproline in HCl. Artery and construct segments (length ~ 5 mm) were cut into pieces no larger than 1.0 mm^2 prior to colorimetric collagen quantification. Total collagen per wet mass of each sample was calculated from the hydroxyproline standard curve. Paired measurements of standards and experimental samples taken in triplicate varied less than 5%.

Medium was collected from each chamber at the termination of culture and evaluated for soluble elastin content using a Fastin Elastin Assay kit [35–37] (kit F2000; Biocolor Ltd., Carrickfergus, UK) following kit instructions after centrifugation to remove tissue fragments, cells, and other insolubles. Samples of unused culture medium incubated with uncultured scaffolds for 10 days were evaluated as a negative control. Elastin concentration in culture medium from the scaffold chambers was calculated from the α -elastin standard curve.

Tissue samples were evaluated for insoluble elastin content using a Fastin Elastin Assay kit (kit F2000) after acid hydrolysis of the tissue to destroy all other proteins, including soluble elastin. Construct and scaffold segments (length ~ 5 mm) were cut into pieces no larger than 1.0 mm^2 and digested with oxalic acid and heat at least three times. Elastin concentration in the supernatant was measured using the kit instructions, and total elastin per wet mass of the sample was calculated from the elastin standard curve. For all elastin assays, standard duplicates had means within 5% of one another and sample duplicates varied less than 10% as allowed by kit instructions.

2.9. Statistical analysis

Results are expressed as mean \pm standard deviation. Statistical significance ($p < 0.05$) was determined by one-way analysis of variance and a Tukey–Kramer post-hoc test.

3. Results

3.1. Process yields, scaffold properties, and cellular confluence

Scaffolds fabricated using a heat-shrinkable mandrel and hyaluronic acid-coated glass tubing (type C scaffolds) were comparable to earlier scaffolds in their yield (Fig. S1) and porosity (Fig. S2) and demonstrated advantages in geometry (Fig. S3), mechanical properties (Fig. S4), and culture time required for SMC confluence (Fig. S5). The yields for PGS and PLGA type C scaffolds were not significantly different ($97\% \pm 13\%$ and $93\% \pm 18\%$ of the scaffolds were usable respectively). Scaffold wall thickness did not vary significantly between PGS and PLGA scaffolds, which were $282 \pm 18 \mu\text{m}$ and $290 \pm 17 \mu\text{m}$ respectively. Porosities were not significantly different and were $84.6 \pm 0.6\%$ for PGS scaffolds compared to $84.2 \pm 0.9\%$ for PLGA scaffolds. Luminal surfaces of PGS and PLGA scaffolds appeared similar (Fig. 1A,B), including

microstructural features that would be encountered by cells during initial adhesion and subsequent migration and proliferation (Fig. 1C,D). SMCs were similarly confluent on the luminal surfaces of engineered arterial constructs based on PGS or PLGA (designated respectively as PGS constructs and PLGA constructs) on day 10 of culture (Fig. 1E,F).

3.2. Macroscopic and histological appearance

Radial and longitudinal compaction of PGS scaffolds was noticeable by day five. Radial and longitudinal compaction of PLGA scaffolds was noticeable by day three and began to inhibit maintenance of luminal flow by day five. PGS constructs retained their scaffolds' cylindrical geometry (Fig. 2A, Fig. S6). Porcine carotid arteries contained dense circumferential bands of cells and extracellular matrix (ECM) proteins organized within the artery wall (Fig. 2B). PGS constructs had concentrations of cells and proteins at the luminal and abluminal surfaces and cells scattered throughout the scaffold walls (Fig. 2C). The distribution of cells and proteins in PLGA constructs resembled that of PGS constructs but with greater scaffold compaction (Fig. 2D).

3.3. Construct mechanical properties

During five compression cycles to 50% strain, segments of porcine carotid arteries and PGS constructs showed almost no measurable decrease in maximum force (F_{max}) (Fig. 3A,B). Each segment had nearly identical force-extension curves for all five cycles, indicating that deformation was elastic. In contrast, PLGA construct segments required much greater force for equivalent deformation and strain, and F_{max} decreased with each subsequent cycle (Fig. 3C). The initial compression cycle of PLGA construct segments showed a steady increase in force during platen extension, but subsequent cycles showed abrupt increases in force during late stages of platen extension, a behavior indicative of plastic deformation. Force-extension data of PGS and PLGA scaffolds likewise showed elastic and plastic deformation, respectively (Fig. 3D,E).

The compressive elastic modulus (E_c) of PLGA constructs was significantly higher compared to E_c of all other groups, including

PLGA scaffolds (Fig. 4A). E_c of PLGA scaffolds was significantly higher compared to E_c of porcine carotid arteries, PGS constructs, and PGS scaffolds. When data for arteries and PGS groups were compared independent of PLGA groups, E_c of arteries was significantly higher than E_c of all PGS groups (Fig. 4B). The E_c of PGS constructs was significantly higher than that of the PGS scaffolds. Degradation did not significantly change E_c (Fig. 4) or mass (Fig. S7) for scaffold segments of either PGS or PLGA.

Hysteresis in porcine carotid arteries (Fig. 5A) and PGS constructs (Fig. 5B) during pressure-diameter testing was observed only for the first cycle to each target pressure, with subsequent cycles demonstrating complete elastic recovery. The brittle nature of PLGA constructs prevented cannulation and adequate sealing at cannulae-construct junctions for pressure-diameter testing. Compliance of porcine carotid arteries and PGS constructs were remarkably similar at pressures up to 56 mmHg, the highest burst pressure achieved for the PGS constructs after only 10 days of culture (Fig. 6). Artery segments excised at different distances from the aorta provided a representative compliance range for the porcine common carotid, with artery segments isolated at locations closer to the aorta showing higher compliance. Mean burst pressure for PGS constructs was 27 ± 19 mmHg. In contrast, uncultured scaffolds hold no pressure due to their high porosity, and wet scaffolds have been shown to be significantly weaker ($\sim 15\%$ of tensile strength) compared to scaffolds cultured with SMCs for three weeks [25].

3.4. Construct biological properties

Collagen content of porcine carotid arteries exceeded collagen content of PGS and PLGA constructs cultured for 10 days by more than an order of magnitude (Fig. 7A). Comparison of experimental groups and negative controls showed that all constructs had significantly higher collagen content than uncultured scaffolds and that PLGA constructs contained significantly more collagen than PGS constructs (Fig. 7B).

Soluble elastin concentrations in culture medium collected on day 10 were equivalent for PGS and PLGA constructs and were significantly higher than complete culture medium incubated with uncultured scaffolds (Fig. 8A). However, PGS constructs contained significantly more insoluble elastin than PLGA constructs and uncultured scaffolds, while insoluble elastin content of PLGA constructs did not significantly vary from uncultured scaffolds (Fig. 8B). After only 10 days of culture PGS constructs contained 35% as much insoluble elastin as porcine carotid arteries.

4. Discussion

We have demonstrated that elastomer-based engineered arterial constructs can match the compliance of native arteries (Fig. 6), including elastic recovery (Fig. 5). The tissue of these constructs contains more than one third of the insoluble elastin found in native arteries (Fig. 8B). Although the burst pressure is sub-physiologic, the *in vitro* culture time was only 10 days. Variation in burst pressures of PGS constructs was probably a reflection of how evenly distributed cells and ECM were longitudinally and circumferentially within construct lumens, especially because tubular, porous PGS scaffolds hold no pressure and are significantly weaker than cultured scaffolds [25]. Since the weakest section of the construct wall determined burst pressure, small differences in cell distribution and seeding efficiency would amplify differences in burst pressure. Additionally, lower seeding efficiency would result in a larger percentage of SMCs at the fluid-cell interface in the lumen, exposing a larger fraction of SMCs to non-physiologic shear stress and causing them to proliferate at a lower rate during early

stages of culture [38], further amplifying differences between constructs. Increased culture time and seeding efficiency may increase burst pressures and decrease variation.

PLGA and PGS scaffolds were comparable in their wall thickness, porosity, and luminal microstructure prior to cell culture (Fig. 1A–D). Cellular confluence in the two materials was similar on day 10 (Fig. 1E,F), with differences attributable to unequal scaffold compaction: macroscopically PGS construct lumens were smooth and PLGA construct lumens were increasingly rough during culture. Equal concentrations of SMCs were observed at the lumen and ablumen of PLGA constructs rather than higher concentrations at the lumen as in PGS constructs (Fig. 2B–D). This was most likely due to PLGA scaffold breaches caused by compaction and subsequent through-wall SMC migration and proliferation. However, PGS and PLGA degradation rates appeared to be similar since moduli (Fig. 4) and masses (Fig. S7) of scaffold segments did not change significantly during the 10-day degradation period.

Differences in PGS and PLGA scaffold compaction during culture are most likely due to different deformation modes (elastic or plastic; Fig. 3) and moduli (Fig. 4). As SMCs exert tensile forces on the PLGA microstructure the scaffold is expected to plastically deform, and the cumulative microscopic deformations caused by SMCs over time will likely result in macroscopic scaffold compaction during culture. In contrast, the PGS microstructure is expected to deform elastically and then return to its original conformation as SMCs form new focal adhesions and release others [39,40], thereby allowing the scaffold to retain a macroscopic geometry similar to its original shape during culture. In an environment of dynamic micro-forces collectively capable of compacting a scaffold with E_c on the order of MPa (i.e. PLGA), the ability to elastically deform may be important in retaining macroscopic geometry.

One important contribution of this study is the demonstration that, when cultured in PGS scaffolds but not in equivalent PLGA scaffolds, SMCs co-express collagen and elastin (Figs. 7 and 8B). Co-expression of elastin and collagen is acknowledged as a significant challenge in vascular tissue engineering [41,42], especially in the absence of growth factors. Collagens and elastin are the primary constituents of vascular ECM and key determinants of the mechanical properties of vasculature [41,43,44]. Significant increases in compressive elastic moduli after 10-day SMC culture indicated that SMCs require a time course of only days to produce substantial ECM (Figs. 7 and 8B) and thereby significantly alter scaffold mechanical properties (Fig. 4).

Elastin and collagen content in PGS and PLGA constructs (Figs. 7 and 8B) may have been influenced by material differences such as stiffness, chemical composition of degradation products released into the medium during culture, and surface chemistry encountered at the cell-material interface. Any of these factors, alone or in combination, could influence protein synthesis and incorporation into the ECM as well as subsequent ECM remodeling by SMCs. However, degradation products were aliphatic acids and alcohols for both polyesters and were diluted by relatively large volumes of medium in this study. Initial protein adsorption differences arising from surface chemistry were likely attenuated by cell-mediated protein adsorption and desorption at the surface throughout culture [45–47]. Therefore, scaffold stiffness is most likely the dominant factor causing differences in protein production in PGS and PLGA constructs.

Scaffold stiffness did not alter the amount of soluble elastin released into medium by SMCs (Fig. 8A) but did significantly change insoluble elastin content of engineered vascular tissue (Fig. 8B). These results suggest that SMCs synthesized elastin in both materials but selectively controlled its incorporation into the ECM based on mechanical cues from the environment. It has been proposed that SMCs operate through homeostatic mechanisms to preserve

the mechanical properties of their environment, and that mechanical perturbations caused by compliance mismatch may be the root cause of graft-associated intimal hyperplasia [5]. Therefore, increased incorporation of compliant ECM proteins such as elastin and decreased incorporation of stiffer ECM proteins such as collagen within PGS constructs are likely a result of homeostatic mechanisms coupled with scaffold elasticity.

Pulsatile perfusion of compliant PGS scaffolds at 1.2 Hz (range: 0.5–1.7 Hz) was expected to increase synthesis of collagen, elastin, and some glycosaminoglycans by increasing cyclic stretch of SMCs [16,17,37,48]. One study showed that subjecting SMCs on poly-(glycolic acid) (PGA) or collagen I to cyclic strain at 1.0 Hz increased elastin and collagen synthesis regardless of scaffold material [37]. Other studies have demonstrated that pulsatile perfusion at 2.75 Hz of engineered arterial constructs improved SMC phenotype and construct mechanical properties [16,17]. The perfused constructs possessed sub-physiologic compliance despite using a stiff material (PGA) organized in a compliant fibrous mesh fitted over compliant silicone tubing [16]. The combined results of these studies suggest that the most dominant scaffold property influencing protein synthesis and deposition under dynamic conditions is mechanics and not material. Therefore, differences in protein synthesis and deposition in PGS and PLGA constructs could be attributed mainly to differences in how PGS and PLGA transduce mechanical stimulation rather than scaffold chemistry. Results from previous studies also suggest that, with an appropriate amount of collagen gel coated on synthetic-polymer scaffolds, collagen production could be increased to create engineered arterial constructs with a more balanced ECM profile [49].

5. Conclusion

This work was motivated by the prevalence of coronary heart disease and the fact that graft compliance mismatch reduces long-term patency. When cultured three-dimensionally in tubular, porous PGS scaffolds under cyclic strain for 10 days, adult vascular SMCs co-expressed collagen and elastin, giving rise to engineered arterial constructs with physiologic compliance. PGS constructs contained more than a third of the insoluble elastin content of porcine common carotid arteries. Arteries, PGS constructs, and PGS scaffolds demonstrated elastic deformation and recovery, while segments of PLGA constructs and PLGA scaffolds demonstrated plastic deformation under identical testing conditions. Short-term culture with SMCs significantly increased scaffold stiffness regardless of material and shifted the stiffness of PGS scaffolds closer to that of porcine carotid arteries. Compared to PLGA, PGS promoted elastin deposition by SMCs but attenuated collagen deposition. Soluble elastin concentration in culture medium was equivalent for PLGA and PGS constructs, as were luminal confluence. The creation of a clinically successful tissue-engineered artery requires not only compliance matching but also sufficient burst pressure and the incorporation of a robust and functional endothelium. We have previously demonstrated co-culture of endothelial progenitor cells and SMCs in PGS constructs [25]. The results of this study combined with former studies therefore provide a possible avenue for engineering non-thrombogenic vascular grafts with physiologic compliance.

Acknowledgments

The authors thank Dr. Edward Balog for providing porcine tissues, Dr. Rudy Gleason for access to his compliance-measuring apparatus, and Daniel Howell, William Wan, and Julia Raykin for experimental assistance. We are grateful to Drs. Stephen Hanson

and Monica Hinds for providing baboon arteries for cell isolation and to Dr. Robert Nerem for insightful discussions.

Sources of Funding: Supported by grant R01HL089658-01 from the National Institutes of Health (National Heart, Lung and Blood Institute) and grant 0730031N from the American Heart Association and Jon Holden DeHaan Foundation.

Appendix

Figure with essential colour discrimination. Fig. 2 of this article is difficult to interpret in black and white. The full colour images can be found in the on-line version, at doi:10.1016/j.biomaterials.2009.11.035.

Appendix. Supplementary material

Supplementary data associated with this article can be found, in the online version, at doi:10.1016/j.biomaterials.2009.11.035.

References

- [1] Rosamond W, Flegal K, Furie K, Go A, Greenlund K, Haase N, et al. Heart disease and stroke statistics – 2008 update: a report from the American Heart Association Statistics Committee and Stroke Statistics Subcommittee. *Circulation* 2008;117:e25–146.
- [2] Daemen J, Serruys PW. Optimal revascularization strategies for multivessel coronary artery disease. *Curr Opin Cardiol* 2006;21:595–601.
- [3] Desai ND, Fremes SE. Radial artery conduit for coronary revascularization: as good as an internal thoracic artery. *Curr Opin Cardiol* 2007;22:534–40.
- [4] Suma H. Arterial grafts in coronary bypass surgery. *Ann Thorac Cardiovasc Surg* 1999;5:141–5.
- [5] Kassab GS, Navia JA. Biomechanical considerations in the design of graft: the homeostasis hypothesis. *Annu Rev Biomed Eng* 2006;8:499–535.
- [6] Trubel W, Moritz A, Schima H, Raderer F, Scherer R, Ullrich R, et al. Compliance and formation of distal anastomotic intimal hyperplasia in Dacron mesh tube constricted veins used as arterial bypass grafts. *ASAIO J* 1994;40:M273–8.
- [7] Sarkar S, Salacinski HJ, Hamilton G, Seifalian AM. The mechanical properties of infrainguinal vascular bypass grafts: their role in influencing patency. *Eur J Vasc Endovasc Surg* 2006;31:627–36.
- [8] Fei DY, Thomas JD, Rittgers SE. The effect of angle and flow rate upon hemodynamics in distal vascular graft anastomoses: a numerical model study. *J Biomech Eng* 1994;116:331–6.
- [9] Abbott WM, Megerman J, Hasson JE, L'Italien G, Warnock DF. Effect of compliance mismatch on vascular graft patency. *J Vasc Surg* 1987;5:376–82.
- [10] Sonoda H, Takamizawa K, Nakayama Y, Yasui H, Matsuda T. Coaxial double-tubular compliant arterial graft prosthesis: time-dependent morphogenesis and compliance changes after implantation. *J Biomed Mater Res A* 2003;65:170–81.
- [11] Okuhn SP, Connelly DP, Calakos N, Ferrell L, Pan MX, Goldstone J. Does compliance mismatch alone cause neointimal hyperplasia. *J Vasc Surg* 1989;9:35–45.
- [12] Stewart SF, Lyman DJ. Effects of an artery/vascular graft compliance mismatch on protein transport: a numerical study. *Ann Biomed Eng* 2004;32:991–1006.
- [13] Hofstra L, Bergmans DC, Hoeks AP, Kitslaar PJ, Leunissen KM, Tordoir JH. Mismatch in elastic properties around anastomoses of interposition grafts for hemodialysis access. *J Am Soc Nephrol* 1994;5:1243–50.
- [14] Sterpetti AV, Cucina A, Randone B, Palumbo R, Stipa F, Proietti P, et al. Growth factor production by arterial and vein grafts: relevance to coronary artery bypass grafting. *Surgery* 1996;120:460–7.
- [15] Kaushal S, Amiel GE, Guleserian KJ, Shapira OM, Perry T, Sutherland FW, et al. Functional small-diameter neovessels created using endothelial progenitor cells expanded ex vivo. *Nat Med* 2001;7:1035–40.
- [16] Niklason LE, Abbott W, Gao J, Klagges B, Hirschi KK, Ulubayram K, et al. Morphologic and mechanical characteristics of engineered bovine arteries. *J Vasc Surg* 2001;33:628–38.
- [17] Niklason LE, Gao J, Abbott WM, Hirschi KK, Houser S, Marini R, et al. Functional arteries grown in vitro. *Science* 1999;284:489–93.
- [18] Campbell JH, Efendy JL, Campbell GR. Novel vascular graft grown within recipient's own peritoneal cavity. *Circ Res* 1999;85:1173–8.
- [19] Roeder R, Wolfe J, Lianakis N, Hinson T, Geddes LA, Obermiller J. Compliance, elastic modulus, and burst pressure of small-intestine submucosa (SIS), small-diameter vascular grafts. *J Biomed Mater Res* 1999;47:65–70.
- [20] L'Heureux N, Paquet S, Labbe R, Germain L, Auger FA. A completely biological tissue-engineered human blood vessel. *FASEB J* 1998;12:47–56.
- [21] L'Heureux N, Dusserre N, Konig G, Victor B, Keire P, Wight TN, et al. Human tissue-engineered blood vessels for adult arterial revascularization. *Nat Med* 2006;12:361–5.

- [22] Gao J, Crapo PM, Wang Y. Macroporous elastomeric scaffolds with extensive micropores for soft tissue engineering. *Tissue Eng* 2006;12:917–25.
- [23] Crapo PM, Gao J, Wang Y. Seamless tubular poly(glycerol sebacate) scaffolds: high-yield fabrication and potential applications. *J Biomed Mater Res A* 2008;86:354–63.
- [24] Gao J, Ensley AE, Nerem RM, Wang Y. Poly(glycerol sebacate) supports the proliferation and phenotypic protein expression of primary baboon vascular cells. *J Biomed Mater Res A* 2007;83:1070–5.
- [25] Gao J, Crapo P, Nerem R, Wang Y. Co-expression of elastin and collagen leads to highly compliant engineered blood vessels. *J Biomed Mater Res A* 2008;85:1120–8.
- [26] Wang Y, Ameer GA, Sheppard BJ, Langer R. A tough biodegradable elastomer. *Nat Biotechnol* 2002;20:602–6.
- [27] Chen QZ, Bismarck A, Hansen U, Junaid S, Tran MQ, Harding SE, et al. Characterisation of a soft elastomer poly(glycerol sebacate) designed to match the mechanical properties of myocardial tissue. *Biomaterials* 2008;29:47–57.
- [28] Wang Y, Kim YM, Langer R. In vivo degradation characteristics of poly(glycerol sebacate). *J Biomed Mater Res A* 2003;66:192–7.
- [29] Murphy WL, Dennis RG, Kileny JL, Mooney DJ. Salt fusion: an approach to improve pore interconnectivity within tissue engineering scaffolds. *Tissue Eng* 2002;8:43–52.
- [30] Hsu YY, Gresser JD, Trantolo DJ, Lyons CM, Gangadharam PR, Wise DL. Effect of polymer foam morphology and density on kinetics of in vitro controlled release of isoniazid from compressed foam matrices. *J Biomed Mater Res* 1997;35:107–16.
- [31] Ho ST, Hutmacher DW. A comparison of micro CT with other techniques used in the characterization of scaffolds. *Biomaterials* 2006;27:1362–76.
- [32] Peterson LH, Jensen RE, Parnell J. Mechanical properties of arteries in vivo. *Circ Res* 1960;8:622–39.
- [33] Strauss BH, Chisholm RJ, Keeley FW, Gotlieb AI, Logan RA, Armstrong PW. Extracellular matrix remodeling after balloon angioplasty injury in a rabbit model of restenosis. *Circ Res* 1994;75:650–8.
- [34] Woessner Jr JF. The determination of hydroxyproline in tissue and protein samples containing small proportions of this imino acid. *Arch Biochem Biophys* 1961;93:440–7.
- [35] Joddar B, Ramamurthi A. Elastogenic effects of exogenous hyaluronan oligosaccharides on vascular smooth muscle cells. *Biomaterials* 2006;27:5698–707.
- [36] Hoerstrup SP, Kadner A, Breymann C, Maurus CF, Guenter CI, Sodian R, et al. Living, autologous pulmonary artery conduits tissue engineered from human umbilical cord cells. *Ann Thorac Surg* 2002;74:46–52.
- [37] Kim BS, Nikolovski J, Bonadio J, Mooney DJ. Cyclic mechanical strain regulates the development of engineered smooth muscle tissue. *Nat Biotechnol* 1999;17:979–83.
- [38] Ueba H, Kawakami M, Yaginuma T. Shear stress as an inhibitor of vascular smooth muscle cell proliferation. Role of transforming growth factor-beta 1 and tissue-type plasminogen activator. *Arterioscler Thromb Vasc Biol* 1997;17:1512–6.
- [39] Yang MT, Sniadecki NJ, Chen CS. Geometric considerations of micro- to nanoscale elastomeric post arrays to study cellular traction forces. *Adv Mater* 2007;19:3119–23.
- [40] Lemmon CA, Sniadecki NJ, Ruiz SA, Tan JL, Romer LH, Chen CS. Shear force at the cell–matrix interface: enhanced analysis for microfabricated post array detectors. *Mech Chem Biosyst* 2005;2:1–16.
- [41] Patel A, Fine B, Sandig M, Mequanint K. Elastin biosynthesis: the missing link in tissue-engineered blood vessels. *Cardiovasc Res* 2006;71:40–9.
- [42] Isenberg BC, Williams C, Tranquillo RT. Small-diameter artificial arteries engineered in vitro. *Circ Res* 2006;98:25–35.
- [43] Gleason RL, Hu JJ, Humphrey JD. Building a functional artery: issues from the perspective of mechanics. *Front Biosci* 2004;9:2045–55.
- [44] Silver FH, Horvath I, Foran DJ. Viscoelasticity of the vessel wall: the role of collagen and elastic fibers. *Crit Rev Biomed Eng* 2001;29:279–301.
- [45] Opas M, Dziak E. Adhesion, spreading, and proliferation of cells on protein carpets: effects of stability of a carpet. *In Vitro Cell Dev Biol* 1991;27A:878–85.
- [46] Grinnell F. Focal adhesion sites and the removal of substratum-bound fibronectin. *J Cell Biol* 1986;103:2697–706.
- [47] Altankov G, Grinnell F, Groth T. Studies on the biocompatibility of materials: fibroblast reorganization of substratum-bound fibronectin on surfaces varying in wettability. *J Biomed Mater Res* 1996;30:385–91.
- [48] Leung DY, Glagov S, Mathews MB. Cyclic stretching stimulates synthesis of matrix components by arterial smooth muscle cells in vitro. *Science* 1976;191:475–7.
- [49] Kim BS, Nikolovski J, Bonadio J, Smiley E, Mooney DJ. Engineered smooth muscle tissues: regulating cell phenotype with the scaffold. *Exp Cell Res* 1999;251:318–28.